Journal of Mining Engineering and Research. 1 (1): 16-34. June, 2019 **www.j-miner.com**
doi:10.35624/jminer2019.01.03

Assessment on the hydrogeological condition of an open pit mine based on piezometric measurements

M. Morales, K. Panthi, R. Rostad
Norwegian University of Science and Technology (NTNU), Trondheim, Norway.

K. Holmøy
SINTEF Byggforsk, Trondheim, Norway.

K. Botsialas
Geotechnical Engineer, Egersund, Norway.

ABSTRACT: Understanding groundwater and flow pattern behavior in a given mine site is generally based on accepted theory related to flow through porous granular media. The existence of discontinuities within the rock mass alters the accepted hydraulic behavior being the joint profile and aperture variability a challenge when designing an open pit mine. In this regard, groundwater interaction with the rock mass is the key variable that influences mining slope design and monitoring. This manuscript studies and analyses the geotechnical perspective of an open pit mine and carries out a comprehensive assessment on the groundwater behavior of an open pit mine in a hard rock environment. The analysis is carried out using data gathered from piezometers and correlating the findings with the structural model of the mine. A comparison of the analysis with the results of previous investigations like hydraulic testing and mapping of the mine site are presented comprehensively. The authors propose the concept of receding time for a better understanding of the drainage capability of a given discontinuity (or a set of them) and its importance in assessing groundwater behavior of the pit slope. Discussions are also made on how groundwater flow can be locally modified by slope scale structures and what are the potential consequences there may have for overall slope stability.

1 INTRODUCTION

The importance of effective management of water in open pit mining increases while pit slope design continues deeper below the groundwater elevation. A hydrogeological model is among the key three components; i.e. structural, rock mass and hydrological, in the geotechnical modelling of an open pit slope. Groundwater design in slope management frequently requires that analysis and decision-making are made based on understanding the rock mass behavior in the mine site. In this matter, the geological and structural complexity of an open pit slope environment complicates the evaluation of the groundwater conditions.

It is well known fact that water pressure reduces the stability of the slopes due to reduced shear strength of potential failure surfaces and increasing the forces that induce sliding (Read and Stacey, 2009). In an environment where temperature decreases regularly below water freezing point, freezing of ground water can cause wedging in the water-filled joints. Freezing of surface water on slopes can also block drainage paths resulting in a build-up of pressures in the slope, which considerably reduces the stability.

To include ground water into slope design two possible approaches in obtaining data for distribution of water pressures within a rock mass must be considered (Wyllie and Mah, 2004):

1. Deduction of the ground water flow pattern from consideration of the hydraulic conductivity of the rock mass and sources of ground water.
2. Direct measurement of water levels in boreholes or wells, or of water pressure by means of piezometers installed in boreholes.

This manuscript deals with hydrogeological issues on stability on a hard rock mining environment. It deals first with the interpretation of hydrogeological information gathered from piezometers and compares against the results of hydraulic testing in the boreholes. The results of this comparison are then weighed against geological structural features in the mine. Finally, the manuscript assesses the implications of the hydrogeological characteristics in the

evaluation of potentially unstable zones of the open pit area.

The research is part of DePOPS (Decisive Parameters for Open Pit Slopes), which is an innovation research project aimed to find out which factors are most important for stability of hard rock open pit walls.

2 CONSIDERATIONS OF HYDROGEOLOGICAL FACTORS

The flow on hard rock environments has been described by Billeaux and Feuga (2013) as two dimensional voids of mechanical origin (such as cracks, fissures and joints of any size) governing groundwater behavior to the extent that it is often said that rock mass hydraulics is in large part the hydraulic of fractures. In this sense, conductivity and roughness are the most important parameters into the fracture hydraulics. Here, conductivity accounts for the characteristics of the infilling material, and joint roughness and aperture are related to flow modes, and thus affects the conductivity. Holmøy (2008) described also groundwater flow into hard rock environments being dependent on discontinuities such as joints and their permeability.

2.1 *Hydraulic Conductivity*

As mentioned before, in hard rock environments groundwater flows predominately along high hydraulic conductivity discontinuities. This flow is also explained because of the very low primary hydraulic conductivity of most intact rock. Therefore, as the hydraulic properties of these rocks are mainly controlled by fracturing, these are also referred as fractured rocks. Unlike sedimentary rock environments, hard rocks generally represent anisotropic and heterogeneous media.

The flow of water through fractures and fissures in rock is often simplified to that of the determination of the equivalent hydraulic conductivity of an array of parallel, smooth, clean discontinuities (Davis, 1969). The evolution of fracture flow behavior and the applicability of Darcy's law was studied by Lee and Farmer (1993) by means of two parallel glass plates with apertures as tight as 0.2 mm. The formula was previously found to be applicable to fractures with apertures as small as 0.2 μm by Romm (in Zeigler 1976). Witherspoon et al (1980) found the law to be unsuited for assessing tight rough fractures and for rough fractures in a high normal stress field (also in Lee and Farmer, 1993). In this sense, Brown (1987) noted a reduction in the accuracy of cubic law estimates when fracture surfaces became closely spaced, with flows about half of that expected from the application of cubic law model. He also established that Reynolds equation is valid in calculating flow, a statement later proved theoretically by Zimmerman and Bodvarsson (1996). The law was considered valid for natural rough uneven and open discontinuities as narrow as 4 μm by Iwai (1976) and Witherspoon et al. (1980). From all the investigations, it is clear that fracture surface roughness can significantly affect the linearity of flow but, nonetheless, laminar and viscous flow is often approximated to flow between smooth parallel plates. In such cases, the highest equivalent hydraulic conductivity for a fracture system is given by the cubic law. The cubic law accepts that the average flow rate of any given fracture is proportional to the cube of aperture, which can be derived from the Navier-Stokes equation:

$$K \approx \frac{ge^3}{12vb}, \quad (1)$$

Where g is the gravitational acceleration (9.81 m/s^2), e and b are the discontinuity aperture and spacing, and v is the coefficient of kinematic viscosity of the fluid.

On the other hand, the lowest equivalent hydraulic conductivity occurs for infilled discontinuities, and is given by relating aperture and spacing to the conductivity of the fracture:

$$K = \frac{eK_f}{b} + K_r \quad (2)$$

Where K_f is the hydraulic conductivity of the filling and K_r is that of the intact rock. The term K_r is included in Equation (2) to account for the condition where there is flow in both the intact rock and along the discontinuities.

Representing the effect of primary and secondary porosity is a critical but difficult problem in the calculation process of an equivalent rock mass conductivity. The interconnections between rock discontinuities and their spacing, aperture size, orientation and roughness decide the porosity and permeability of rock masses. Open joints not filled with weathered or crushed rock material form potential passage for groundwater movement, but their permeability is greatly reduced when filled with clay. The use of the cubic law is an effective way of calculation for most engineering purposes, except where fractures are

considerably rough or pressure gradients are large. In these circumstances laminar flow behavior can be replaced by transitional or turbulent flows.

2.2 *Aperture and roughness*

It has been previously declared that the cubic law can lose soundness at large pressure gradients or under very rough surfaces, i.e. non-laminar flow, or where fractures are particularly tight, given the effect of capillarity. Increases in roughness diminish the assumption of plate parallelism in a two-dimensional space. In three dimensions, these results in an extra growth of flow path tortuosity in the plane of fracture itself. Laboratory experiments conducted by Witherspoon et al. (1980) showed that the back-calculated hydraulic aperture is less than the actual mechanical aperture under saturated conditions along a rough surface or in small aperture fractures. This was also proved by Cook et al. (1990). This discrepancy rises with increasing roughness under laminar flow conditions. Barton et al. (1985) established an empirical relationship, Equation (3), that links hydraulic aperture e_h, mechanical aperture e_m, and the roughness profile (JRC) for the condition $e_m \mid e_h$ (apertures are measured in μm):

$$e_h = \frac{e_m^2}{JRC^{2.5}} \tag{3}$$

Equation (3) was derived from laboratory data and assess empirically for non-parallel flow through a rough surface. The relationship between JRC and fracture roughness, as described by the standard profiles proposed by ISRM (1978), provides a useful association to hydraulic and geotechnical behavior. The influence of roughness on hydraulic flow can be measured using the Darcy's and Poiseullle's laws as shown in Equation (4):

$$Q = \frac{e_h^3 w}{12\mu}\left(\frac{dh}{dx}\right) \tag{4}$$

This led to the conclusion that fractures roughness promotes frictional losses and reduces the flow rate of groundwater seepage. By combining the Barton et al. (1985) expression with the parallel plate equation for intrinsic permeability, the following equation can be developed in terms of mechanical aperture and JRC:

$$K = \frac{e_m^2}{12JRC^5} \tag{5}$$

From Equation (5) it is possible to see that surface roughness increasingly impacts upon the continuity and thickness of the fluid boundary layer at the fracture wall, leading to increased flow path tortuosity and the development of localized turbulence. This behavior causes the discrepancy between the actual or mechanical aperture of a fracture and the hydraulic aperture that would be back-calculated from Poiseuille's law, when the hydraulic gradient and the flow rate are known. This characteristic is demonstrated by the relationship shown in Equation (3). In practice, smooth fracture JRC, i.e. low roughness, can often be approximated by $e_h = e_m$. The effect of increased roughness by the reduction in intrinsic permeability is that roughness impacts more severely on K for small aperture defects (by more than four orders of magnitude). This is explained because permeability (in parallel plate model) calculated using the mechanical aperture (e_m) for the condition $e_m = e_h$ and comparing it with the permeability calculated using the real corresponding e_h.

3 LOCAL ENVIRONMENT

The open pit mine is in an area where precipitation happens throughout all the year, with typical values ranging from 90mm to 280mm in a single month. Maximum daily precipitation may reach 75mm in 24 hours. Daily temperatures may be as low as -12^o during winter and also reach over zero. Therefore, freezing and thawing periods might be also important to consider in stability analyses. The open pit itself has a length of approximately 3 km and the current depth is close to 240 meters from the top. 4 lakes are found in the surrounding of the pit. The mining activity is planned to extend the depth of the pit significantly from what it is at present. Consequently, short-, medium- and long-term stability is a crucial matter for this mine.

3.1 *Geology*

The area of study is often described as a great anorthosite in which the ore body is intruded, with the structure of the ore becoming increasingly complex in the east, as xenoliths of anorthosite are present within the ore body. The anorthosite, which is located within the ore body or in the contact zones, typically shows more alteration than in the surrounding rock mass of

the pit slope. The typical dip and dip direction of the contact zone between anorthosite and ore is 50-60/220. Two major diabase dikes crosscut the ore body at WNW-ESE direction. These dikes have straight appearance and dip almost vertical. Many studies have shown that there are areas of heavy alteration that are linked to fractures and fault systems at the mine site, in both ore body and anorthosite.

3.2 *Lineaments*

It has been described before in hard rock areas that movement and occurrences of groundwater depends mainly on the secondary porosity and permeability resulting from folding, faulting, fracturing, etc. The most obvious structural features that are important from the groundwater point of view are the main discontinuities. Discontinuities like faults, joints or cracks developed generally due to tectonic activities provide important clue on surface features and are responsible for infiltration of surface run off into sub-surface and also for movement and storage of groundwater (Subbu Rao et al., 2001). Morales et al (2017a) have shown that there are six different main discontinuities orientations in the mine area, which are correlated with the regional pattern of lineaments. In this manner it was also possible to distinguish six different fracture systems (FS) in the site, as shown in Figure 1.

4 PIEZOMETRIC INFORMATION

An electric piezometer consists of a deflecting diaphragm and a porous filter separated by a small reservoir of water. Deflections of the diaphragm are detected using a vibrating wire or a strain gauge and are converted to an equivalent pressure using a suitable calibration. The piezometer is installed into a fully grouted

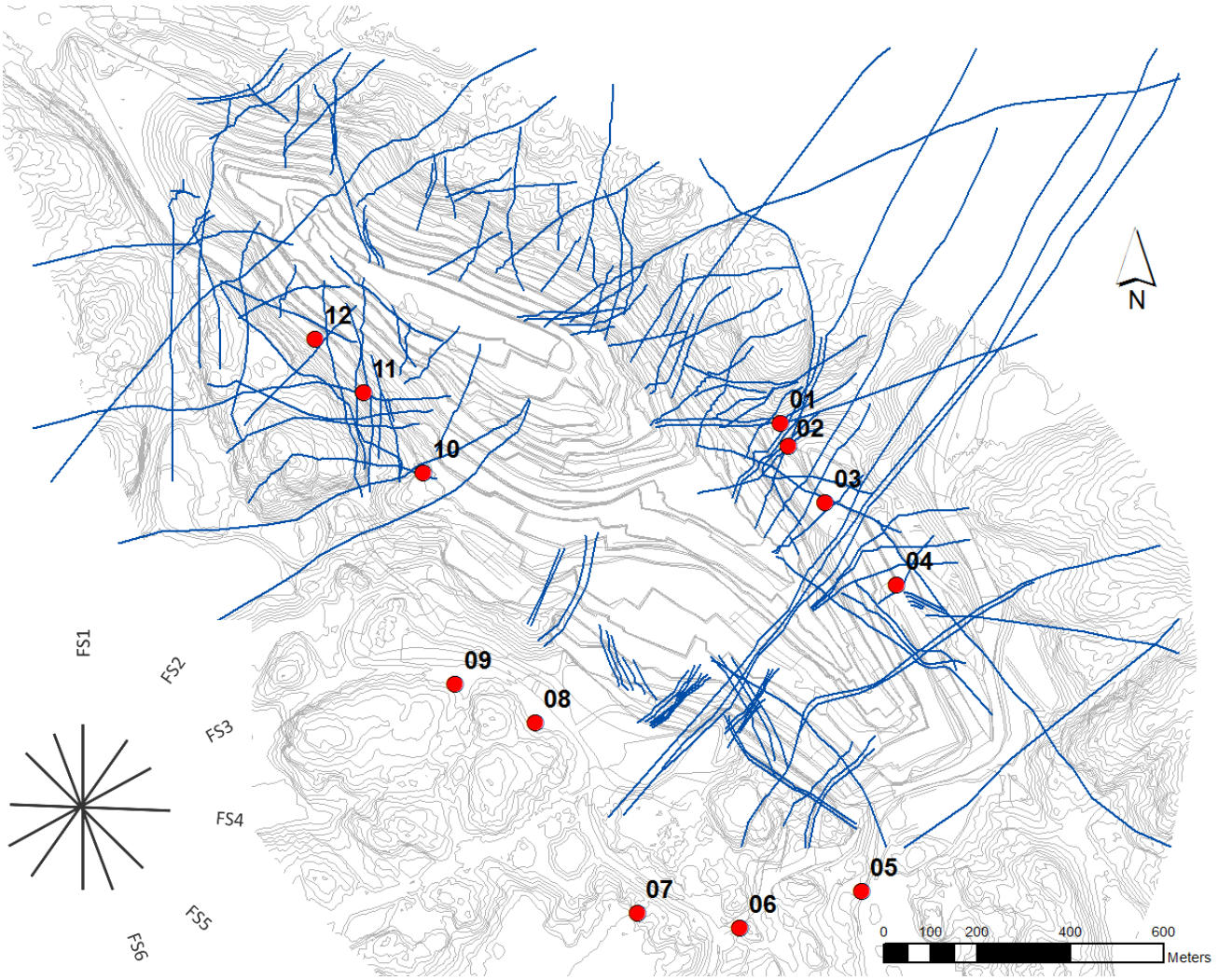

Figure 1: Discontinuities surface traces of the mine area and borehole positions (modified from Morales et al, 2017).

Table 1: Number and depth of piezometers (in meters) in each borehole

Sensor	Borehole 01	02	03	04	05	06	07	08	09	10	11	12
A	34	51	79	41	56	50	92	41	41	61	80	55
B	118	120	136	165	111	103	207	142	165	106	112	108
C	262	-	160	-	155	316	320	260	-	173	202	183
D	-	-	-	-	-	-	-	327	-	240	-	239

borehole. The advantages of fully grouted boreholes into the collection of piezometric data have been documented by Mikkelsen and Green (2003). Water from the ground reaches into the reservoir and causes the diaphragm to deflect until the pressure inside the reservoir is the same as the pore water pressure in the ground at the elevation of the porous filter. If a piezometer is installed above the prevailing ground water table, the pore pressure in the medium could be negative and the water in the piezometer will tend to be drawn out of the reservoir. If this happens, air can eventually form inside the piezometer and it will not function reliably.

A thorough evaluation of the construction or maintenance operation sequence and the geotechnical features of the host rock mass is essential to plan an intelligent and effective piezometric monitoring program (USBR 6515, 2015). For the purpose of hydrogeological characterization at the open pit mine, a total of 36 piezometers were installed, distributed into 12 vertical near-to-vertical boreholes, both in the hanging and footwall (Figure 1). Each borehole hosts 2-4 piezometers that record pressure data every 4 hours. Boreholes are designated with numbers from 01 to 12, and the piezometers inside are indexed by characters A, B, C or D, being A the closest to the surface. Table 1 shows the number of piezometers and depths of installation (in meters) inside each borehole.

4.1 *Pressure increase*

It is well known that low persistence joints that are not connected to the slope face may develop high transient water pressures. On the other side, joints with greater persistence that are connected to the slope face allow water to drain, limiting the water pressure to build up. It should be noted that blast damage is one of the causes of a denser networks of fractures close to the slope face. However, Wyllie and Mah (2004) stated that any improvement in slope stability due to the increase in conductivity is probably out-weighed by the decrease in stability resulting from blast damage to the rock.

To quantify the net pressure increase (this is considering only pressure variations), it is possible to fix a reference time where the maximum pressure caused by any given rainfall event occurs (at t=0). This value is defined as the net pressure increase (Figure 2, point B) by its difference to the pressure recorded by the corresponding piezometer before the rainfall. The net pressure increase is proposed as an indicator of areas where water pressures might play a more active role in slope stability.

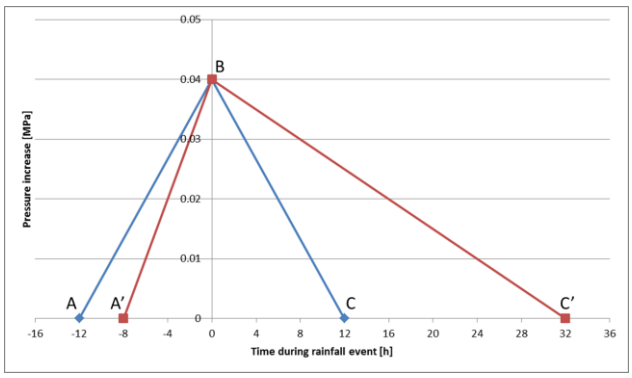

Figure 2: Proposed graph for pressure increase and receding time.

4.2 *Response time*

The response time is the elapsed time between the start of the pressure increase after a rainfall event and the subsequently recorded maximum pressure at the piezometers of the instrumented borehole. Points A and A' in Figure 2 represent the time were pressure increase starts after the rainfall event and point B is the peak of pressure development. Hence, the response time is the time length it takes for a piezometer to "react" to a rainfall event and maximum pressure recorded. At this mine, automatic piezometer data record is

set for 4 hours and therefore the minimum response time corresponds to 4 hours.

An analysis on the response times of piezometers in each rainfall event will define permeability conditions of the discontinuity sets, which is crucial in identifying the potential stability condition of the pit slope. It is, however emphasized here that a faster response time does not necessarily mean that it will lead to slope failure. Nevertheless, a difference in the behavior of piezometers inside the same borehole will help to identify on how conductive the joints are, which is of importance for the assessment of the slope failure.

4.3 *Receding time*

The concept of receding time aims to characterize the behavior of any given piezometer in terms of drainage capacity of the discontinuity sets that lie between the two piezometers. It is understood as the time it takes for the pressure to decrease from peak pressure, or maximum pressure, and return to the initial pressure, or the pressure measurement where the increase of pressure took place, before the rainfall event. It is well known that faults consisting clay and chemically weathered rock may have low conductivity and act as ground water barriers behind which high water pressures could develop. In contrast, faults comprising crushed and broken rock may have high conductivity and act as a drain. It is expected that an assessment of the receding time on either side of the fault will indicate the presence of these features.

Considering only pressure variations again, it is possible to fix a reference time where maximum pressure occurs at t=0 at any given rainfall event, (Figure 2, point B). The points C and C' represent the time where the registered pressure is equal or lower than the initial pressure. The pressure increase at times C and C' is equal or less than zero, and the time values reflects how long does it take to the discontinuity to come back to the initial pressure conditions, before the rainfall event. The authors propose that if the ratio of gradients between pressure built up and receding pressure is near to -1 (case ABC) then it is possible to conclude that water flows freely in the joint, while ratios lower than -0.5 might indicate that a feature is acting as a water barrier (case A'BC').

5 METHODOLOGY

The assessment of hydraulic conditions in the study area is based on many sources of information: jointing distribution from the structural model of the mine (Morales et. al, 2017a), groundwater level measurements from boreholes, piezometric data, rainfall data, joints roughness profile measurements in the mine area, and results from hydraulic testing. The proposed methodology takes in account all the different sources of information in order to assess the hydraulic conditions in the open pit mine and their relationship with the pressure increase, response and receding times registered by piezometers. The following flowchart (Figure 3) illustrates the proposed method:

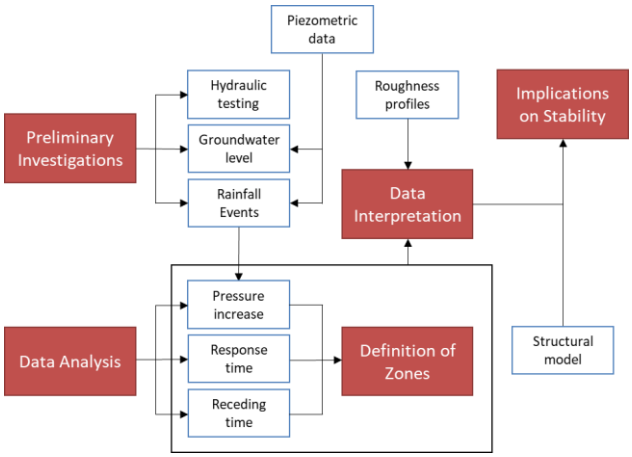

Figure 3: Methodology of the study.

The methodology presented on the figure above can be summarized as follows:

1. Initial assessments: preliminary investigations with data acquired previously from the mine site. These are basically:
   a. Definition of rainfall events. The goal is to isolate the biggest 30 events in terms of total precipitation and rain fall intensity, and then analyze the behavior of the piezometric data in each of these events. It is supposed that intensity and amount of precipitation is in direct relationship with the pressure increase inside the discontinuities. Therefore, the analysis of rainfall events that are big enough embraces the idea of the worst-case scenario.
   b. Set a reference groundwater level from seepage points, measurements from piezometers and short boreholes, and recharge zones (such as lakes) in the periphery of the mine.

   c. Results of previous investigations from hydraulic testing in boreholes.
2. Analysis of piezometric data: data gathered from piezometers is analyzed in order to assess trends/correlations. Analysis for information at each piezometer are done in:
   a. Pressure increase during rainfall events.
   b. Response time during the beginning of each rainfall event.
   c. Receding time behavior after rainfall events.
3. Definition of analysis zones based on the type and spatial distribution of data. This step includes analyses and systematization of information in steps 3 to 5. The zones are then defined based on the quality and type of information.
4. Interpretation of piezometric data: including the findings of the previous step and the preliminary investigations, assessments are done in:
   a. Comparative study of results derived from pressure increase, response time, and receding time against results of hydraulic testing and hydrogeological conditions observed during field work.
   b. Estimation of hydraulic conductivity class to each feature identified from the previous analysis, based on the classes proposed in the hydraulic testing report.
   c. Interpretation of results of piezometric analysis and their relationship with the main structural features of the mine.
5. Assessment of the implications of the hydrogeological conditions of the mine into potential instabilities in the slopes.

6 INITIAL ASSESSMENTS

6.1 *Selection of rainfall events*

A database of rainfall every 15 minutes, recorded from June 2014 until November 2016, was provided by the mining company. Throughout the time lapse of collected rainfall data, there has not been any lack of precipitation. Anyway, the monthly accumulated rainfall reveals an outline of two precipitation seasons; namely high precipitation season and "low" precipitation season. The high precipitation season lasting over August until February, and the low precipitation season in the remaining months, from March throughout July.

In order to classify a rainfall event, the following parameters have been considered: duration, accumulated precipitation, and intensity (amount over duration). Previous studies performed by the mining company takes in account the product between average rainfall intensity and accumulated rainfall as one method of classification. This method favors long-lasting rainfall events as the accumulated rainfall varies greater than the average rainfall intensity between events. As these recordings were subject for analyzing, the criteria for rainfall event determination follows the Hydrological Observatory of Athens' definition (Papathanasiou et al., 2013; Vessia et al., 2014), which considers that when more than 0.4 mm of rainfall is observed by at least two stations within a 10 min period and ends when no station records are greater than 0.2 mm of rainfall for at least 2 hours. The problem with this definition at the present case becomes complicated since the interval of piezometric data record is 4 hours. Therefore, in this study, the authors propose the concept of "core intensity" as a way to start searching for rainfall events. The search therefore starts trying to find the highest amount of precipitation in any interval of 4 hours. Then the events are expanded backwards and forward following the recommendations of the Hydrological Observatory of Athens'. This method allows having rainfall events with a minimum theoretical length of 4 hours, time enough to have at least one piezometric measurement inside the duration of the event. Finally, the biggest 30 events were considered for the detailed analysis. Core intensities ranged from to 5.8mm/h to 10.8mm/h, while the average intensity throughout the complete event ranged between 1.9mm/h to 5.9mm/h.

6.2 *Reference groundwater level*

The first assessment is the reference groundwater level. It gives an idea of how ground water might or might not be present on the pit slope. Presence of water in fractures yields a reduction of shear strength of the discontinuity surface and may develop a potential failure surface. Groundwater aggravates weathering and under aggressive circumstances over longer time the rock mass quality is reduced considerably leading to reduce the stability of the pit wall. Therefore, ground water condition is an important factor when studying the stability of an open pit slope.

In addition to precipitation, other water sources in an open pit are the recharges from lakes, reservoirs, rivers, brooks and smaller water bodies close to the pit and they can unite to

charge up the ground water level. Information coming from smaller boreholes drilled in 2016 where only the water level was recorded allowed us to interpret an approximate water table (Figure 4). The interpreted phreatic line shows an acceptable upper limit where water can accumulate. There are not any boreholes in the bottom of the pit to confirm the height of the ground water level. The surrounding water bodies (lakes and swamps) were used to define the absolute maximum height of the ground water level as boundary conditions. The data was loaded into Leapfrog and an interpolation was made and boundary conditions were adjusted manually. Areas where the line is in front of the pit wall in Figure 4 are interpreted as prone to show seepage in the face of the slope.

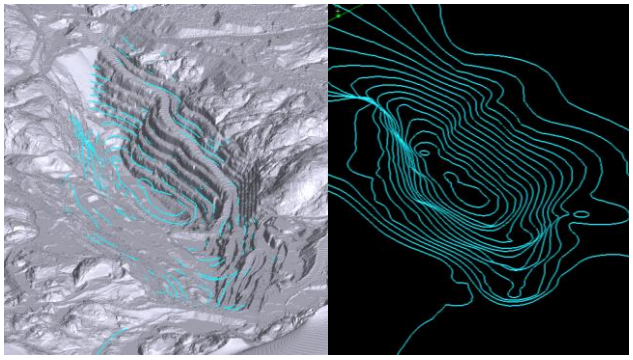

Figure 4: Groundwater lines compared to pit walls (left) and as gradient distribution (right).

6.3 *Results from previous hydraulic testing*

The use of hydraulic testing is a widespread practice in mining industry. In hard rock environments, Maréchal et al. (2004) have successfully applied pumping tests for the evaluation of hydraulic properties in fractured granites, allowing the characterization of the complexity of flows through joints.

A variety of tests were performed in all the boreholes as indicated in Figure 1 (with exception of borehole number 11) by Ruden AS during May and June of 2014. All the boreholes follow a vertical or near-to-vertical direction. The tests included top packer, single packer, double packer, pump, flowmeter, and slug test. Not all the tests were done in each borehole, being this defined by experts from the mining company and the testing consultant by taking account a structural geophysical logging aimed to identify fracture zones and zones of weakness along the entire borehole logging sections. Spinner flowmeter logging was performed in several boreholes under pumping and ambient conditions depending on local feasibility. Flowmeter logging provided information about the presence and flow rate of detected water bearing fractures. Hydraulic testing was also performed in several boreholes. Table 2 provides a general overview of testing on each position.

Table 2: Distribution of hydraulic testing in each borehole.

Borehole	Flowmeter	Hydraulic Test	Lugeon Test
01	X	X	X
02		X	X
03	X	X	X
04		X	X
05		X	X
06	X	X	X
07	X	X	X
08	X	X	X
09	X	X	X
10	X	X	X
11			
12	X	X	X

The objective of the testing was to identify and characterize the water-bearing fracture zones, joints, fractures and/or fissures, and determine the hydraulic parameters of those fracture zones (transmissivity, hydraulic conductivity, permeability etc.). The total aperture of the identified fracture zone was also defined based on geophysical investigations. A summary of the water bearing zones is presented in Table 3. Dip and dip directions of each fracture zone is derived based on the assessment of the results from geophysical investigations.

Table 3: Water bearing fractures from hydraulic testing.

Borehole	Depth [m]	Dip [deg]	DipDir [deg]	Aperture [mm]
03	79.8	31	164	70
03	116.0	62	226	52
03	136.1	48	239	79
03	160.5	47	239	66
05	52.0	24	312	52
08	142.5	68	229	112
08	147.6	77	61	157
08	326.7	48	227	116
08	327.3	62	225	134
08	327.6	58	226	120

08	328.2	64	225	60
09	178.4	65	65	48
09	209.2	56	66	38
09	269.7	42	58	69
09	269.9	49	46	49
10	23.7	49	45	27
10	23.7	48	56	20
10	23.8	47	70	19
10	77.7	66	82	76
10	174.8	83	46	25
12	9.3	64	55	71
12	18.2	44	50	18
12	26.6	48	38	29
12	56.7	52	66	30
12	182.0	78	273	11
12	182.3	70	276	19
12	182.5	71	268	22
12	182.8	76	255	9

Due to the spatial distribution of boreholes (Figure 1), the testing program was done dividing the mine in 3 zones. The first group included four boreholes (01, 02, 03 and 04) drilled on the east side of the mine on the footwall side. The second group included five boreholes drilled on the south and southwest part of the mine (05, 06, 07, 08 and 09). The third group included three boreholes located on the western side of the mine (10, 11 and 12).

High conductivity zones were identified in all three groups of boreholes (Figure 5). In group 1, four water bearing zones were identified, all of them in borehole 03. The main fracture zone (79.8m) is found in the middle of the dike, which is also the one having the highest hydraulic conductivity (very high). Fractures at 136.1m and 160.5m have about half hydraulic conductivity of the upper one (high), and the fracture at 116m has lower permeability (also classified as high).

In group 2, water bearing zones were identified in boreholes 05, 08 and 09. The water bearing zone identified in borehole 05 was interpreted to have considerable permeability due to recharge from a near swamp (very high conductivity). Fracture zones at borehole 08 were defined to contain considerable water amount and have high permeability. The fractures zones (probably all in the host rock or at the host rock/mineral contact) were defined to have an "elastic behavior", which means that their size can increase with the water pressure and store more water for example after a rainy period. Water bearing zones at 142.5m and 326.7-328.2m have similar orientation and dipping angle to the contact between the host rock and the ore. Finally, 3 water bearing fracture zones were identified in borehole 09, defined to have very high hydraulic conductivity with a capacity to store considerable water.

In group 3, borehole 10 and 12 were identified to have water bearing zones. The zones identified in borehole 10 are having a low conductivity at depths of 23.7m and 77.7m. The hydraulic conductivity increases at moderate

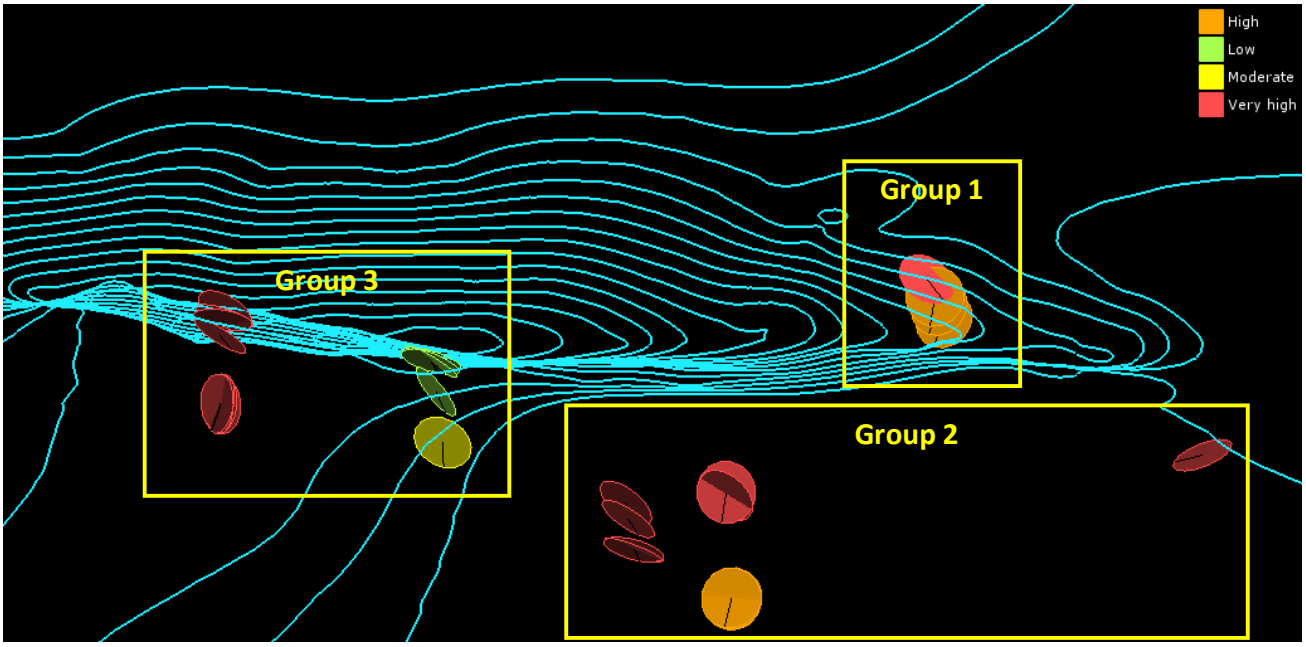

Figure 5: Spatial distribution of water bearing zones and proposed conductivity classes.

depth of 174.8m. On the other hand, all the water bearing zones in borehole 12 were described to belong to the very high conductivity class.

In order to identify structural features linked to water bearing zones, an analysis based on the jointing direction of geophysical logging data was done. In group 1, borehole 03 was identified to intersect the diabase dike (the upper weathered part), while the 01 and probably 02 stopped in the dike. Borehole 04 was not interpreted to have any connection with the dike. The very high conductivity fracture zone is approximately in the middle of the dike and about parallel to it (dipdir 164°), but its dip angle is smaller. The lower three zones are more or less perpendicular to the dike and the main fracture zone and have steeper dipping angles (52-79/235) and are linked to the contact zone between ore and host rock. It was concluded that important water bearing zones and water flow are found only in the fractures of the dike or in the fractures intersecting the dike. The upper weathered part of the dike was interpreted to form a confined aquifer, which can conduct a lot of water, and the lower as un-weathered and homogeneous rock mas without big fractures (as possible to see in the log of borehole 01 below 274.5 m).

Analysis of boreholes in group 2 showed that water bearing fractures zone in borehole 05 between 51.5-57.5 m (24/312) has connection with the shallow water system of nearby swamp. Boreholes 08 and 09 receive their recharge through the fracture zones east (40-70/060). These fractures have high permeability and can convey a lot of water from the background to the pit. The fractures at 40-70/230 both in the upper and lower part were interpreted to be linked with the contact zone between the host rock and the ore, since the location, dip angle and orientation is in line with the values in the geological model of the mine, as suggested in an internal report. These values are equivalent to the ones found in boreholes in group 1 (57-79/235), in the contact zone of the footwall.

On group 3, the interpretation of logging data showed that only borehole 12 intersects the dike (the lower un-weathered, fresh part) while the other boreholes does not have any connection with it. Due to the proximity of the mine walls and by visual inspection it was possible to identify the host rock/ mineral contact in these boreholes with the analysis of well logs. Water bearing zones in borehole 10 are subparallel to the mine slope (47-66/060), and probably connected to each other. It must be noted that this orientation is the same that the ones in boreholes 08 and 09. Borehole 12 tests and observations revealed that this well intersects two water systems: a temporary aquifer of the hillside in the host rock, and a deep aquifer of the dike. After a rainy period, fractures between 9-56.7m (45-65/060) can divert water into the pit.

As a summary, the hydraulic testing revealed three major structural features dominating the water flow in the mine. Fractures in the 40-70/060 in the hanging wall (both in groups 2 and 3), the contact zone between ore and host rock at 40-80/230 in groups 1 and 2, and the diabase dike in groups 1 and 3.

7 INTERPRETATION OF PIEZOMETRIC DATA

7.1 *Pressure increase*

In general, high pressure increase in a discontinuity surface may be caused either by the fact that the discontinuity is not daylighting to the face or the infilling material has restricted water to drain freely. Only sensors in borehole group 3 showed high values of pressure increase in relation to the rest of the boreholes. Boreholes 10, 11 and 12 of group 3 show highest pressure increase upon rainfall event. In addition, borehole 09 also shows high pressure increase in the top sensor (Figure 6). This behavior may have been caused by the presence of fractures with good communication and relatively rapid flow of water. This postulate may also be confirmed with a quick receding time as well. Pressure increases in boreholes 01 to 09 are not as high as on boreholes 10 to 12, which indicated the presence of a more active area (in terms of pressures build up). On the other hand, fractures that do not daylight at the slope face may also lead to a pressure increase. As shown in Figure 6, the two boreholes showing the highest pressure increase are boreholes 11 and 12. Borehole 11 has the highest pressure increase in the top sensor 11A and in the bottom sensor 11C. These measurements are somewhat special relative to their surroundings and match with two sensors in borehole 12, sensors 12B and 12C.

The pressure built up at sensors 11A and 11C may not have same sources of water supply, as the bottommost sensor 11C has lower pressure increase than sensor 11A. It is likely that the major pressure increases in sensor 11A and 11C originate from different discontinuity sets. In borehole 12, sensors 12B and 12C have the greatest pressure increase (Figure 6). 12B and

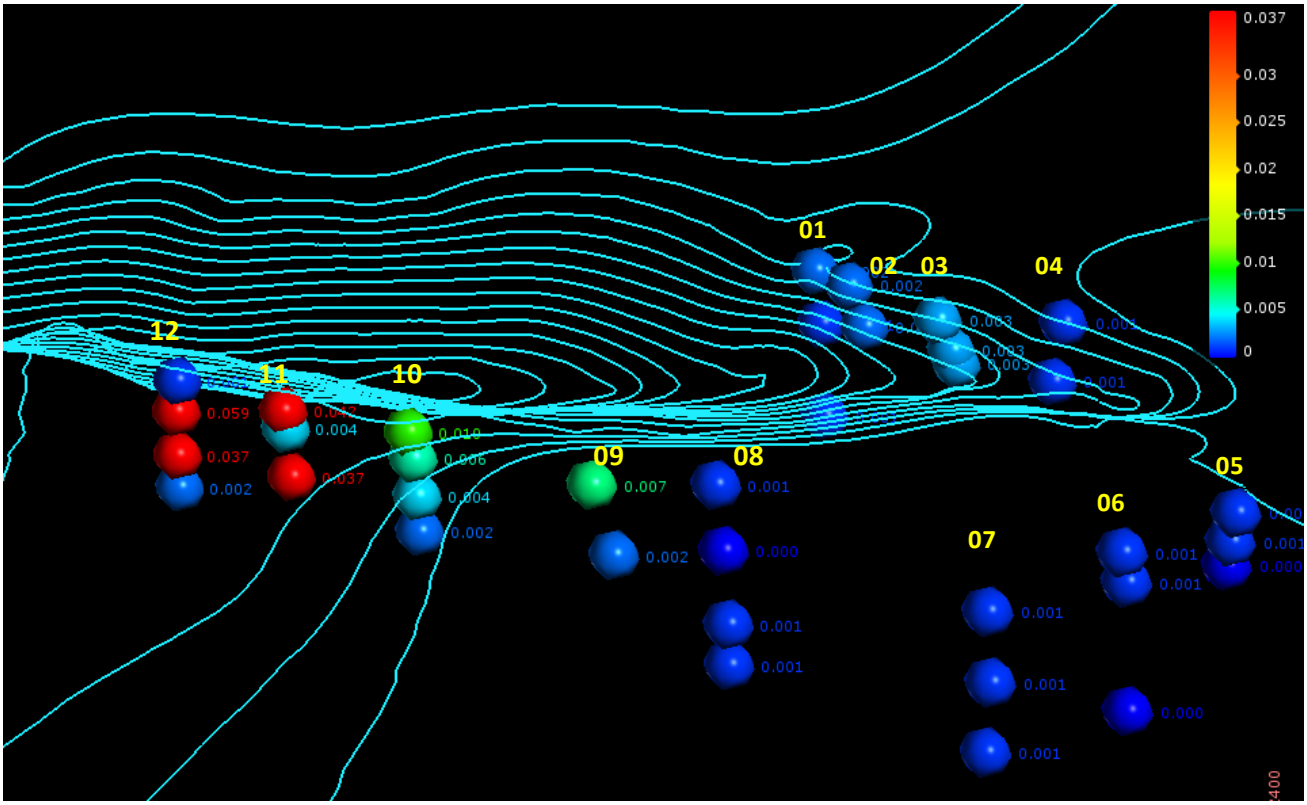

Figure 6: Net pressure increase per piezometer (in KPa).

12C are enclosed by sensors 12A and 12D, which do not model a pressure increase to the same extent. Sensors 12B and 12C exhibit the same behavior as the case depicted by sensors 11A and 11C.

Similarly, the top sensor in both boreholes 09 and 10 exhibit different behavior compared to the ones in the bottom part (Figure 6). Pressure increase in both sensors 09A and 10A are in the range of 0.007 to 0.010 KPa, while the bottom sensor reaches to 0.002 KPa in both cases. This is the indication that it is linked to the same feature in both cases. This may also be correlated to the presence of a water barrier between sensors in the top and bottom, not allowing water to flow to the bottom sensors, thus allowing pressure increase in the top. On the other hand, as Figure 6 indicates, sensors 01 to 08 do not show a noticeable difference among the pressure increase recorder by each piezometer.

7.2 *Response time*

The response time of each piezometer was analyzed in order to define response classes that are believed to help understand the trends or specific behavior of reaction time of each sensor during each rainfall event. Data was first filtered in order to avoid misleading data sources or outliers that may distort the analysis set. It is found that response times ranged from 0.4 to 56.8 hours, which allowed defining 5 response classes categorized as from very slow to very quick (Table 4). A sudden change of response time between piezometers in the same borehole (or a particular behavior within the same group) indicates the presence of a joint of relevant hydraulic characteristics.

Table 4: Response time classes.

Class	Min [h]	Max [h]	Definition
1	-	5.00	Very Quick
2	5.00	10.00	Quick
3	10.00	20.00	Medium
4	20.00	30.00	Slow
5	30.00	100.00	Very Slow

On the boreholes that are positioned in the footwall of the mine (group 1), borehole 01 has the highest variation in the response time within the sensors. The bottom sensor 01C is on average medium to respond compared to the other two sensors having quick response. Regarding borehole 02, being closely positioned to borehole 01, one can assume that these two boreholes should exhibit similar behavior as of 01. However, the top sensor in borehole 02A has medium response time, while 02B responses quick indicating inverted behavior compared to

borehole 01. Borehole 03 has all three sensors in response class medium indicating good homogeneity. Borehole 04 shows medium response time on the bottom sensors and the top sensor responses quick.

In group 2, the borehole with the fastest response time is 05, where the sensor 05A and 05B respond very quickly unlike 5C with quick response time. This is logical since 05C is located deep into the rock mass. Borehole 06 exhibits somewhat differently in character having quick response time at 06A, medium response time at 06B and slow response time at 06C. Borehole 07 does not show a variation within all 3 sensors and have slow response time. In borehole 08, the three uppermost sensors (08A, 08b and 08C) are the slowest one to respond to the rainfall events and can be classified as slow responding sensors. The deepest 08D sensor however has medium time. Finally, sensors at borehole 09 have a medium response time.

Piezometers in group 3 showed interesting behaviors. The two topmost sensors (10A and 10B) at borehole 10 showed a quick response time while the other two (10C and 10D) fall in medium class category indicating more tight joints as one goes deeper into the rock mass. Sensors 11A and 11C if borehole 11 had quick response time, while the sensor in the middle (11B) responded medium. In borehole 12 the topmost (12A) was classified as slow, on the other hand 12B and 12C responded very quickly and sensor 12D as quick.

7.3 *Receding time*

The receding time of the piezometer sensors helps to find out on how the rock mass at the surrounding area behaves hydraulically (Figure 7). The holes belonging to group 1, boreholes 01 and 04 show a receding time in the order of 20-35 hours in all their respective sensors. On the other hand, boreholes 02 and 03 have receding times between 60-80 hours. This may be linked to the structural features influencing on the pattern of water drainage out of the hole.

The boreholes belonging to group 2 indicated interesting characteristics regarding receding times. In borehole 05 the receding time of the bottom sensor 05C is twice as quick compared to 05A and 05B (18 versus 40-45 hours). Almost similar behavior was observed in borehole 06, where sensors 06B and 06C are having receding times of 10 and 18 hours, compare to around 40 hours for the topmost piezometer 06A. The sensor 07B at borehole 07 had a receding time of 32 hours, which is slower in comparison to the sensors 07A and 07C with a receding time of 16 and 5 hours respectively. Borehole 08 has almost similar receding patter as of borehole 07 having top sensors receding at 32 hours, and sensors 08B, 08C and 08D having receding time varying

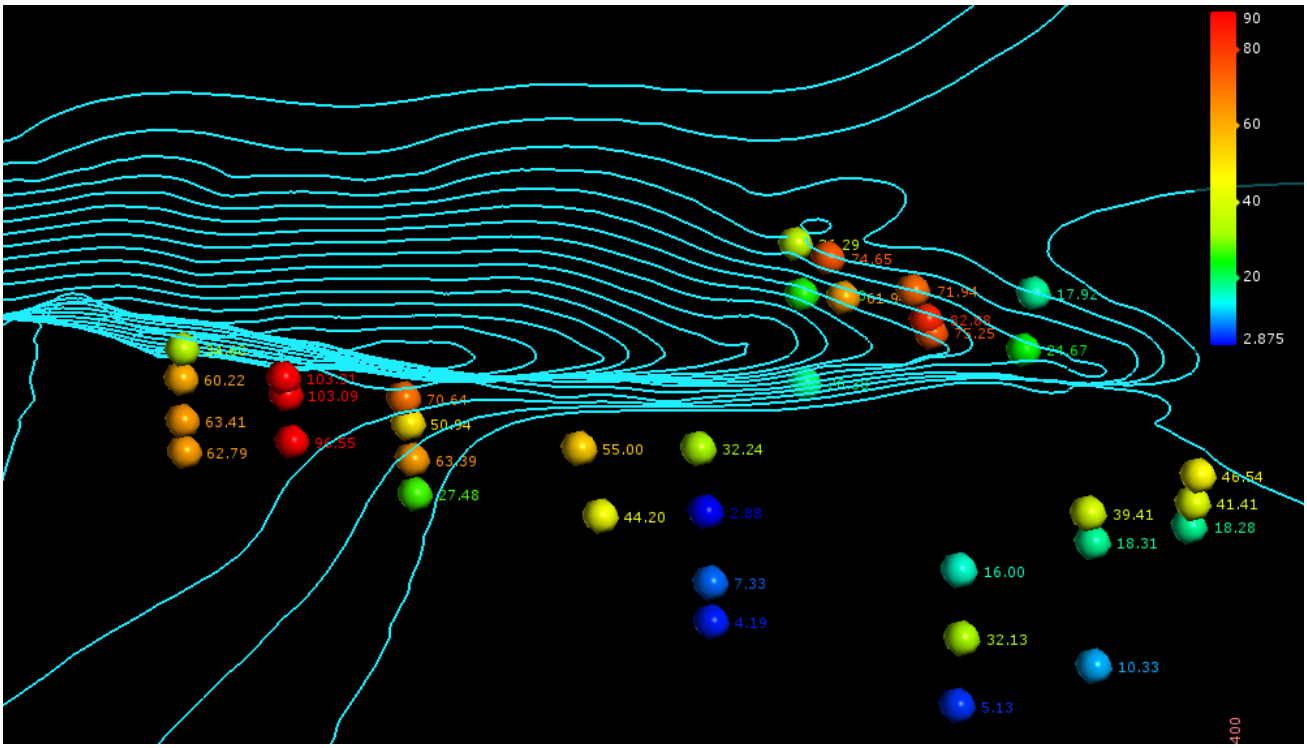

Figure 7: Distribution of average receding time in piezometers.

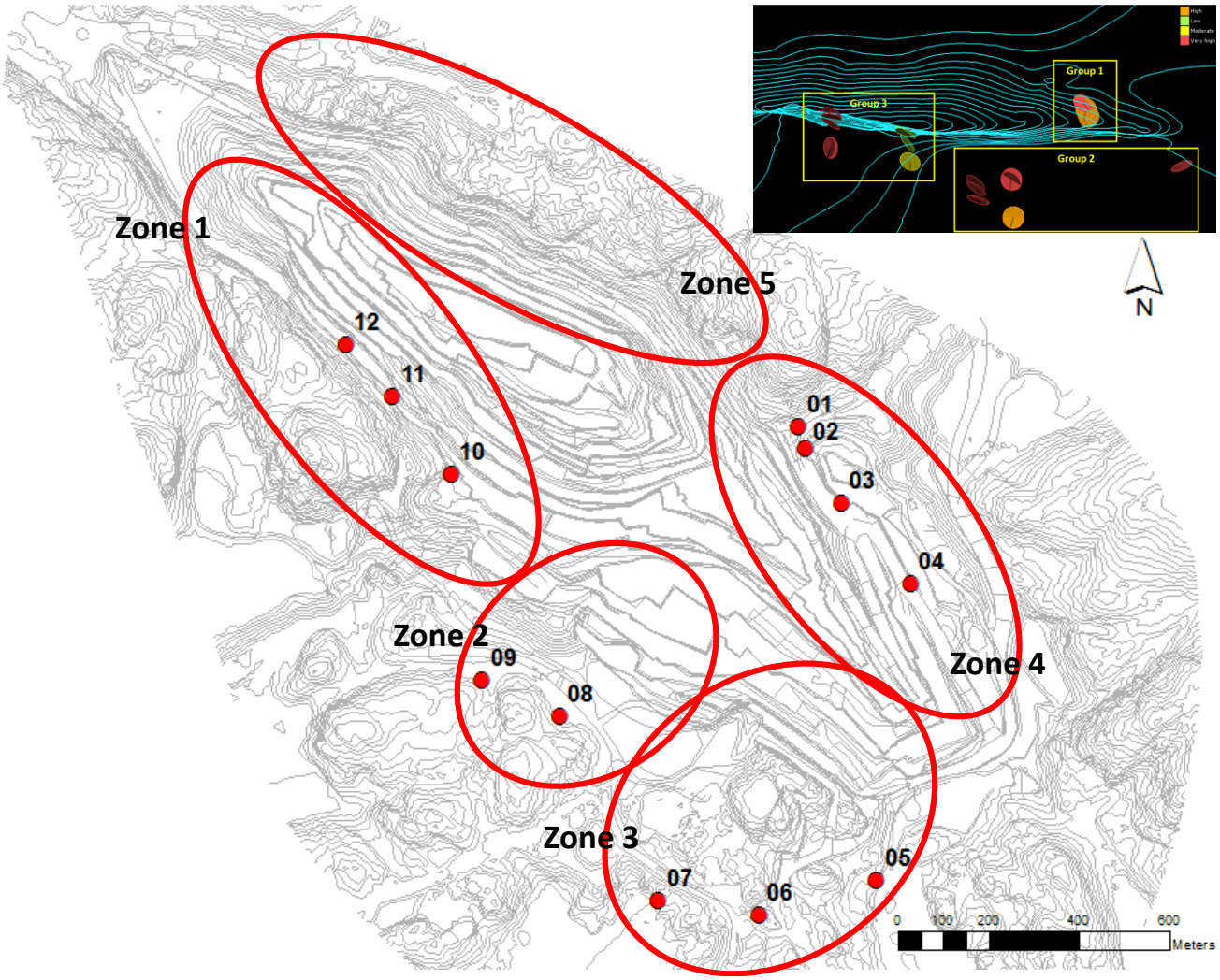

Figure 8: Analysis zones according to field experience and available data. Groups from hydraulic testing are shown in the upper right corner.

at 3-7 hours. Borehole 09 exhibited stable patterns with relatively long receding times of 55 and 44 hours for 09A and 09B sensors, respectively.

Finally, in borehole group 3, borehole 10 shows the same pattern as borehole 08, but with different magnitudes and distribution. The bottommost sensor 10D has a receding time of 27 hours, while 10A, 10B and 10C have 2 to 3 times larger receding time with 76, 50 and 63 hours, respectively. Borehole 11 has unexpectedly longer receding times (exceeding 100 hours) for all three sensors. Finally, borehole 12 shows relatively quicker receding time of 30 hours in sensor 12A, while the three bottom sensors 12B, 12C and 12D are having values in the order of 60 hours, which is relatively long.

8 DEFINITION OF ANALYSIS ZONES

Based on the spatial distribution of boreholes with piezometers installed, quality and type of data and considering state of pressure increase, response time, and receding time, the open pit mine is further divided into 5 different zones (Figure 8). The defined zones are in line with the testing groups defined during the hydraulic testing of the boreholes. Group 2 discussed previously (Figure 5) is further split into two analysis zones (zone 2 and zone 3) and a new zone 5 was introduced to cover the whole area of the mine. At zone 5 neither hydraulic testing was carried out nor were piezometers installed. The data are assigned to four different categories consisting presence of piezometer, hydraulic testing, data on jointing condition, and seepage points. Data on jointing condition are further split into three different categories based on roughness, infilling condition and aperture. A reliability index is assigned to each area based on the extent of data set availability (Table 5). Zone 1 and zone 4 represent boreholes group 3 and group 1, respectively. Zone 2 and zone 3 belongs to the subdivision of boreholes group 2.

Table 5: Information and reliability aspect of each analysis zone.

	JOINTING						
Zone	Piezometer	Hydraulic testing	Roughness	Infilling	Aperture	Seepage points	RELIABILITY
1	X	X	X		X	X	HIGH
2	X	X	X		X	X	HIGH
3	X	X	X		X	X	HIGH
4	X	X	X		X	X	HIGH
5			X		X	X	LOW

9 HYDROGEOLOGICAL ASSESSMENTS

9.1 *Structural evidence*

Figure 9 shows the plan view of the mine area of Figure 1 (left) including the previously defined analysis zones, and the main lineaments mapped from aerial photos (right).

Evidence in the model shows that zone 1 is dominated by the presence of two water bearing planes associated to FS1 and FS5 at 70/270 and 46/058, respectively. The limit between hydraulic units here is defined by a joint derived from a high receding time in piezometer 10A and structural information on borehole 10. The findings have good correlation with what is possible to observe in the field, and also good correlation with a higher pressure increase in sensor 10A compared to 10B, 10C and 10D, as clay filled zones are most likely water barriers and build up the pressures. Figure 10 shows the intersection of the water barrier plane with borehole 10. Quick receding time in sensor 12A is most likely related to the joints with orientation 50/060 corresponding to FS6. This joint system dips towards the pit and daylights at benches over level 140. Same orientation is also observed in the uppermost water bearing zone in borehole 10 (sensor 10A), but receding time here is higher than in borehole 12. This is explained by the proximity of a clay filled discontinuity that acts as a water barrier in the direction FS3 at 65/346. It is possible that the influence of this alteration zone might have extended not only to the plane itself but also to neighboring fractures. This hypothesis is confirmed with slow receding times in sensors 10B and 10C and also a fast receding time in sensor 10D. The same behavior is observed between boreholes 08 and 09 (in zone2) thus defining another alteration zone with similar dip and dip direction than the one defined between boreholes 10 and 12 (Figure 10).

In zone 2, sensors at borehole 09 are located closer to the surface in comparison with other boreholes. It is likely that the rainwater has less distance to reach the sensors at borehole 09 based on assessments on the communication between fractures and sensors. The complex fracture network that present in the mine however indicates the presence of communication from the surface via fractures to the sensors, which allows relatively quick response time.

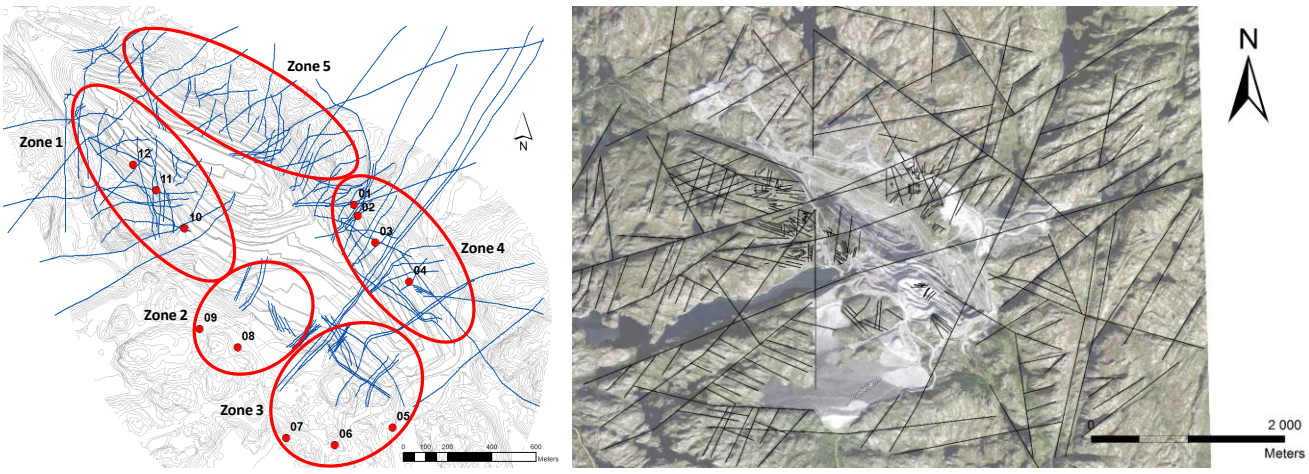

Figure 9: Plan view of boreholes, structures and zones (left), and lineaments (right).

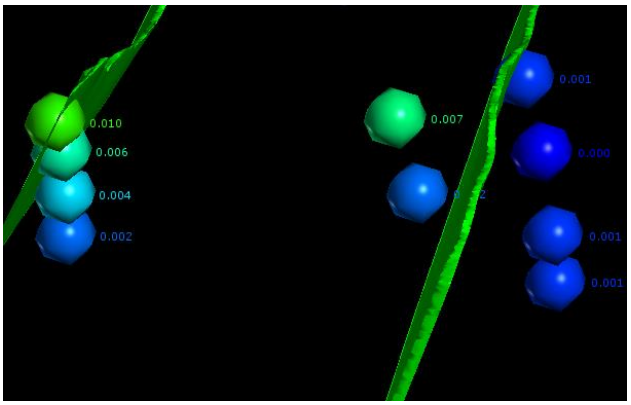

Figure 10: Interpreted water barrier structural planes in boreholes 08 and 09.

Information from sensors in boreholes in zone 3 shows that the main water bearing plane in this area is linked to the contact between ore body and host rock. This explains the erratic behavior both in response and receding time, as the contact surface between both units has been defined as undulating with average direction around 65/220. It is very interesting to note that the same pattern is present in borehole in group 1 (zone 4), especially in borehole 04, leads to the same evidence of a water bearing zone associated to the contact surface.

The structural analysis of boreholes in zone 4 showed that the most important structural features in this area are the diabase dike and the contact between ore body and host rock. As no particularly significant pressure increase was noticed at this zone, the response and receding time may be linked to the flow pattern. Evidence in both cases leads towards differences in pressure measurements between sensors inside boreholes 02 and borehole 03. This difference is explained by the presence of the diabase dike in both cases. It is also evident that sensors in this contact zone show receding times in the order of 60-70 hours, same as the sensors in the same contact zone of the diabase dike in the opposite wall, in borehole 10. Figure 11 shows an overall picture of the most important hydrogeological features in the mine.

9.2 *Hydraulic conductivity assessment*

In order to assess sensitivity of fracture conductivity to aperture and fracture frequency

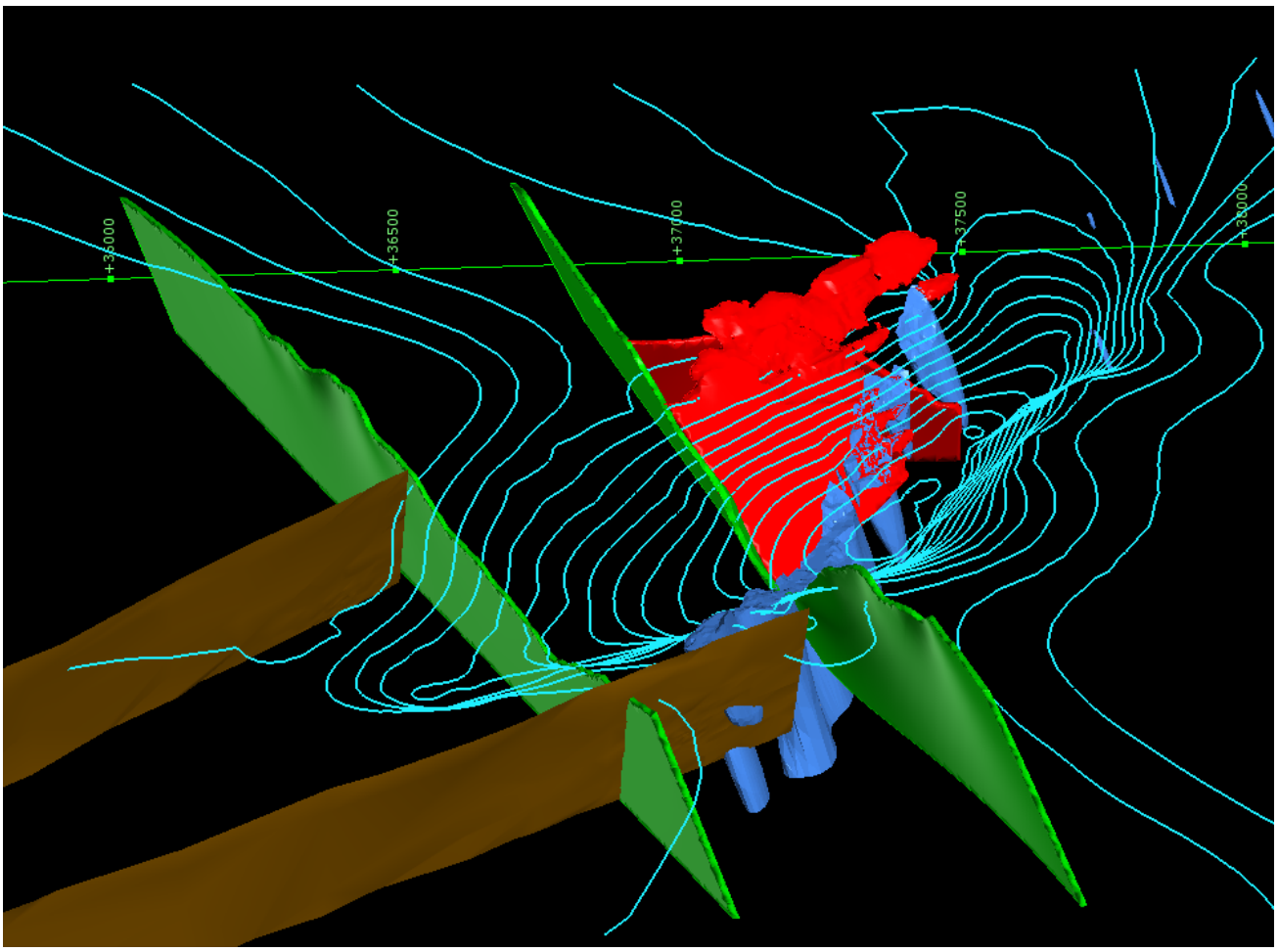

Figure 11: Major hydrogeological features in the open pit.

as defined by Hoek and Bray (1981) a rosette diagram (Figure 12) was introduced. The figure clearly shows that the joints associated to the contact between the host rock and the ore body (NW-SE direction) is water bearing due to their aperture, which is the characteristic of fractures at zone 3 and zone 4. From the diagram is also possible to observe that direction NNW-SSE that corresponds to FS6 has also joint with big aperture. This system is present in zone 1 and zone 2 with dip/dip direction around 45/060 and has been reported as connected to most of the instability events in zone 1 in the past.

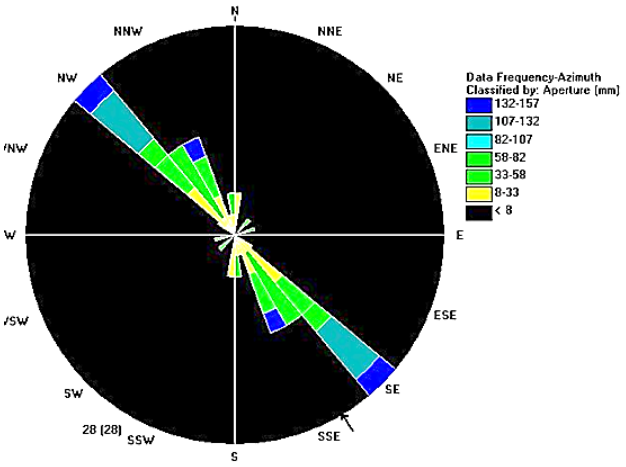

Figure 12: Rosette diagram with aperture for water bearing zones identified by hydraulic testing.

In terms of joint persistence, zone 2 is believed to be enclosed by two clay filled water barriers related to FS3. Average spacing between the main fractures of lineament FS3 is around 400-500 meters (Morales et al, 2017a), which is the widest spacing of all the fracture systems at this mine. Radar monitoring of the area confirms small displacements of a well monitored wedge during rainfall events. Since zone 2 is surrounded by barriers it is logical to assume that high pressures may build up near the barrier planes. As shown in Figure 8 and Figure 9, no borehole is drilled between borehole 09 and 10 (both boreholes intersect one of the barriers at each side), it would be of great advantage to drill and install piezometers in an intermediate location in order to better understand the behavior of this zone.

The Barton and Choubey (1977) relationship shows that for infilled joints, the relevance of roughness depends on the thickness and the strength of infilling material. In this matter, a surface mapping campaign for recording values of dip, dip direction, and JRC, was carried out in the summer of 2016 by Morales (2017b). Joint amplitude measurements were taken along 10, 20 and 100cm profiles and later on correlated to the JRC (Table 6).

Table 6: Average roughness rating and JRC class per fracture system.

Fracture System	Avg. roughness rating within RMR	Avg JRC
FS1	6	16-20
FS2	2	6-10
FS3	6	18-20
FS4	3	8-12
FS5	4	10-14
FS6	3	8-12

The hydraulic test results in borehole 10 identified highly jointed zones corresponding to FS5, which is filled with clay material working water barrier. Borehole 10 intersects the bands including a nearby vertical fractured zone, which crosses FS1 and FS5. This vertical zone is usually filled with clay and has low permeability, meaning a slow to very slow response time class (Table 4) which shows a good correlation with JRC.

Regarding stress distribution, most water bearing structures are usually oriented subparallel to the highest principal stress orientation (Selmer-Olsen, 1971; Holmøy, 2008). A report from the mining company from 1979 shows two locations where stress measurement was carried out and it was reported that the major principal stress was found to be of 6.8MPa and 4.4MPa, respectively. According to the report the orientation of σ_1 is N20E (location 1) and N13W (location 2) and dip at around 4 to 20 degrees towards South. On the other hand, the two major water bearing surfaces are FS6 (45/060 or N30W) and the contact plane between the host rock and the ore body with orientation 50/230 (strike: N40W). Both of these planes seem to have subparallel orientation to the principal stress measurement at location 2 suggesting similarities with the Selmer-Olsen (1971) findings.

10 IMPLICATIONS OF GROUNDWATER ON STABILITY

Morales et al (2017b) have developed a map of potential unstable zones on the mine by calculating the SMR index (Romana, 1985) covering completely the surface slope of the pit. The authors highlighted the effect of groundwater on the slope stability. It is a well-known fact that the pressure built up caused by groundwater decreases the shear strength and increases the potential unstable behaviour of a given slope. In these regards three major structural features were identified to be linked to high groundwater pressure; i.e. the fracture system with the orientation of 40-70/060, the two major discontinuities between zone 1 and 2 (65/345), and zone 2 and zone 3 (70/340). These systems belong to the fracture system and the contact between ore and host rock (40-80/220).

According to Morales et al (2017a) the fracture system at 40-70/060 is considered to be present in two area of the mine, both in the hanging wall (zones 1 and zone 3 in Figure 8). This is in line with the values of SMR calculated in the pit as indicated in Figure 13. Hence, potentially unstable zones are prone to occur in these areas of the mine. These findings are in line with the high pressure increases and low response times found on the top sensors of borehole 10 and borehole 11, which correlates well with the water bearing zones defined by hydraulic testing.

On the other hand, the lower pressure increase in sensor 10A and sensor 09A are explained by the presence of the two structural planes (in red in Figure 13), which are known to have clay bearing weak planes and therefore act as water barriers to groundwater flow. This behaviour is also confirmed by the lower pressure increase in

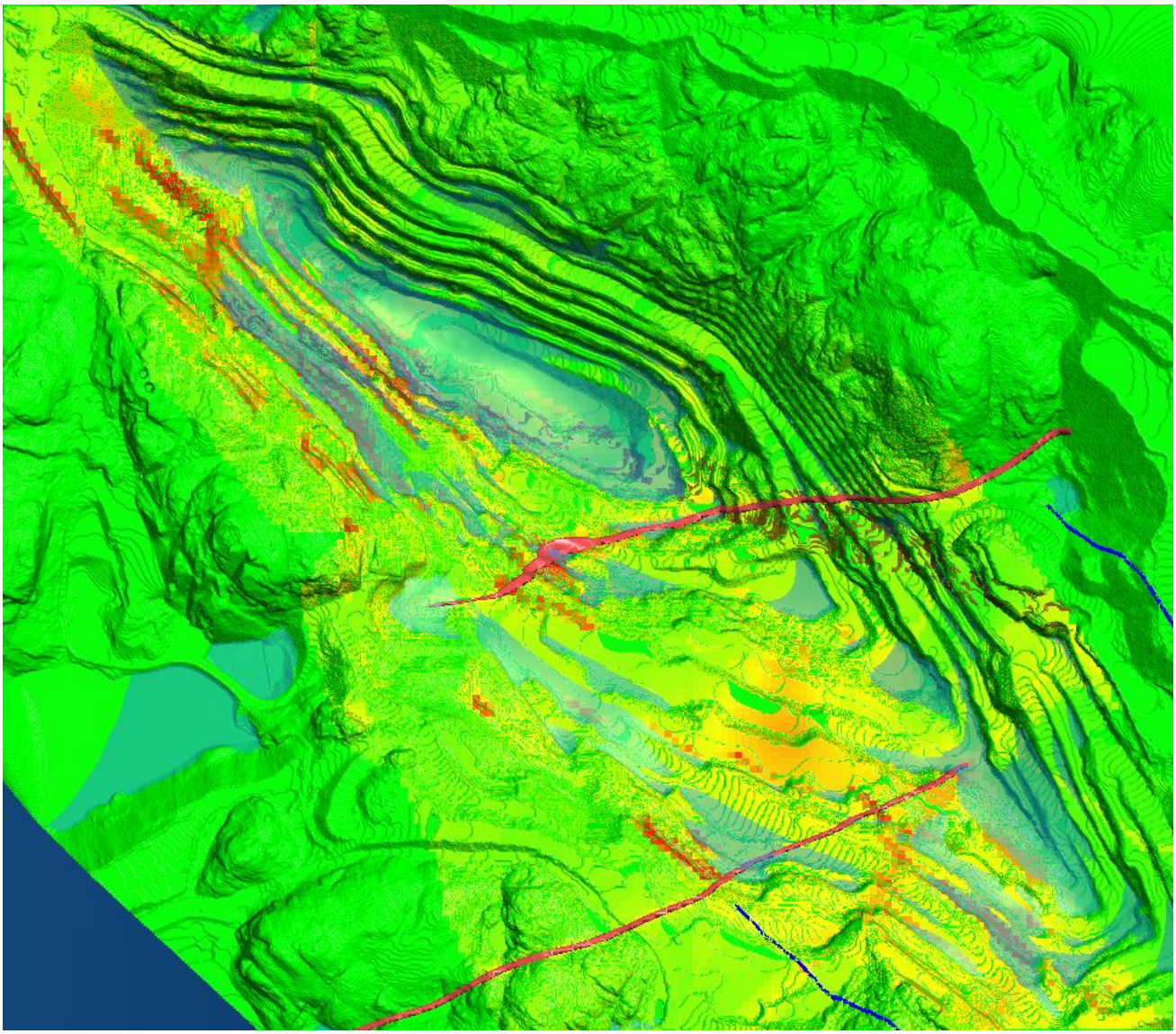

Figure 13: SMR map linked to hydrogeological features.

the bottom sensors of borehole 09 and borehole 10. In addition, longer receding times of both sensors also confirms that the big planes defining a zone where water does not flow freely leading to increase in the pressure and unfavourable regarding stability.

Finally, the contact between ore body and host rock does not represent a risk in terms of orientation to stability, since it dips into the hanging wall and is way behind the footwall. In contrast, hydraulic conditions might favour the flow or divert of water into other minor joints, which may allow pressure to increase. This is also confirmed by the southernmost water barrier plane where the red areas are in the same location (Figure 13).

11 CONCLUSION

The analysis has indicated that it is possible to interpret hydrogeological conditions from piezometric measurements. The response time, pressure increase, and receding time are all connected to the impact from the rainfall events. There is in particular one zone where these characteristics are more prominent than in the rest of the mine; i.e. in the hanging wall area associated with boreholes 10, 11 and 12. Particularly sensitive piezometers within this region are sensors 11A, 11C, 12B and 12C. It is inferred that the occurrence of: (i) quick response time, (ii) greater pressure increase on average, and (iii) a slow drainage represented in high receding time might have impact of stability. In fact, this is the main area for previous unstable events in the mine and the most probable area where there might be stability challenges in the days to come. However, with a denser array of boreholes and sensors, the discovery of similar areas might be detected in other places of the open pit mine. In combination with other models, this hydrogeological interpretation hence can be used as a tool for understand vulnerable areas of pit slope to stability and help enhance safety awareness and make strategy on the remedial measures.

Furthermore, the interpreted major hydrogeological features in the mine are highly correlated to the hydrogeological conditions in hard rock environments, as the water bearing planes are mostly associated to high apertures, low roughness and subparallel orientation to the major principal stress. On the same way, water flow barriers seem to be linked to low apertures and high roughness and are derived from different pressure increases within the same borehole, as explained in 7.1, and receding times higher than usual.

Evidence of past events and present monitoring regarding water bearing zones or barriers has been confirmed with respect to potential stability issues. Joints at 45/060 in the hanging wall are well known to create the geometry of planar failure and also to have caused failures in the past, which is strongly correlated with the presence of water and high apertures and low roughness of these planes.

REFERENCES

Barton. N., Choubey. V (1977) *The shear strength of rock joints in theory and practice*, Rock Mechanics, vol. 10. pp. 1—54.

Barton, N., Bandis, S., Bakhtar, K. (1985) *Strength deformation and conductivity coupling of rock joints*, International Journal of Rock Mechanics and Mining Sciences and Geomechanics Abstracts, vol. 22, no. 3 pp. 121-140.

Billeaux, D., Feauga, B. (2013) *Groundwater in Rock Masses*. Chapter 4 in Engineering in Rock Masses, F.G. Bell, 2013. Elsevier, 592p.

Brown, S.R. (1987) *Fluid flow through rock joints: the effect of surface roughness*. Journal of Geophysical Rsearch, (92). Number B2, pp 1337-1347.

Cook, A.M., Myer, L.R., Cook, N.G.W., Doyle, F.M. (1990) *The effect of tortuosity on flow through a natural fracture*. Rock Mechanics Contributions and Challenge&. in Proceedings of the 31st US Symposium on Rock Mechanics. Balkema, pp. 371—378.

Davis, S.N. (1969) *Porosity and Permeability of Natural Materials*, In: Flow through porous media. DeWeist, Academic Press, New York, pp. 54-89.

Hoek, E., Bray, J.W. (1981), *Rock Slope Engineering* Revised 3rd Edition, IMM London.

Holmøy, K.H. (2008) *Significance of geological parameters for predicting water leakage in hard rock tunnels.* Doctoral Theses at NTNU 2008:291. ISBN 978-82-471-1284-7. 224p.

ISRM (International Society for Rock Mechanics) (1978). *Suggested Methods for the Quantitative Description of Discontinuities in Rock Masses*, In ET Brown (ed.). Part 1. Site Characterization. Rock Characterization Testing and Monitonng: ISRM Suggested Methods. Pergamon Press, Oxford.

Iwai, K. (1976) *Fundamental studies of fluid flow through a single fracture*. PhD thesis. University of Berkeley, USA.

Lee, C.H., Farmer, I. (1993) *Fluid Flow in Discontinuous Rocks.* Chapman and Hall, London, 169p.

Maréchal, J. C., B. Dewandel, K. Subrahmanyam (2004), *Use of hydraulic tests at different scales to characterize fracture network properties in the weathered-fractured layer of a hard rock aquifer,* Water Resour. Res., 40, W11508, doi:10.1029/2004WR003137.

Mikkelsen, P.E., Green, G.E. (2003). *Piezometers in fullt grouted boreholes*. In proceedings of the Symposium

on Field Measurements in Geomechanics,, Oslo, Norway.

Morales, M., Panthi, K.K., Botsialas, K., Holmøy, K.H. (2017a) *Development of a 3D structural model of a mine by consolidating different data sources*. Bulletin of Engineering Geology and the Environment. Accepted and in the process of publication.

Morales, M., Panthi K.K., Botsialas K. (2017b) *Development of a 3 dimensional rock mass model for slope stability assessment*. Bulletin of Engineering Geology and the Environment. Accepted and in the process of publication.

Papathanasiou, C., Makropoulos, C., Baltas, E., and Mimikou, M. (2013). *The Hydrological Observatory of Athens: a state-of-the-art network for the assessment of the hydrometeorological regime of Attica*. In Proc. 13th International Conference on Environmental Science and Technology, pp. 5-7.

Read, J., Stacey, P. (2009) *Guidelines for Open Pit Slope Design*. 512pp. ISBN: 9780643101104, Publisher: CSIRO Publishing.

Romana, M. (1985) *New Adjustment Ratings for Application of Bieniawski Classification to Slopes,* Proceedings of International Symposium on the Role of Rock Mechanics, International Society for Rock Mechanics, Salzburg, pp. 49-53.

Subbu Rao, N. et al. (2001) *Identification of Groundwater Potential Zones Using Remote Sensing Techniques in and around Guntur town, Andhra Pradesh, India*. J. Indian Soc. Remote Sensing, 29(1&2): pp 69-78.

Selmer-Olsen R. (1971), *Engineering Geology – a compendium in engineering geology for civil engineers* (in Norwegian). TAPIR FORLAG, 230p.

USBR 6515, *Procedure For Using Piezometers to Monitor Water Pressure in a Rock Mass. Materials Engineering and Research Laboratory*, code 86-68180, Technical Service Center, Denver, Colorado.

Vessia, G., Parise, M., Brunetti, M., Peruccacci, S., Rossi, M., Vennari, C., and Guzzetti, F. (2014). *Automated reconstruction of rainfall events responsible for shallow landslides.* Natural Hazards and Earth System Sciences, 14(9): pp. 2399-2408.

Whiterspoon, P.A, Wang, J.S.Y., Iwai, K., Gale. J.E. (1980) *Validity of Cubic Law for fluid flow in a deformable rock fracture*. Water Resources Research 16(6):pp 1016-1024.

Wyllie, C. and Mah, W. (2004) *Rock Slope Engineering Civil and Mining.* In: Hoek, E. and Bray, J.W., Eds., Rock slope Engineering, Taylor & Francis Group, London and New York, 431p.

Zeigler, T.W. (1976) *Determination of rock mass permeability*. Technical report S-76-2. US Army. Engineer waterways experiment station, Vicksburg, Miss., 114p.

Zimmerman, R.W., Bodvarsson G.S. (1996) *Hydraulic conductivity of rock fractures.* Transport in Porous Media (23) pp 1-30.